

A Multiband Meanderline Rectenna: Design and Simulation for Enhanced Performance

Vishnu Raghuthaman Nedungadi ^{1*}, Vidhyapriya Ranganathan ²

¹ Dept. of Biomedical Engineering, PSG College of Technology, Coimbatore, Tamil Nadu, India

² Dept. of Biomedical Engineering, PSG College of Technology, Coimbatore, Tamil Nadu, India

Abstract: This research article presents design, simulation and analysis of a novel meanderline microstrip patch rectenna to harvest energy from the 2.4 GHz and 5.0 GHz frequency bands. The research is approached in two stages. In the first stage, a meanderline microstrip patch antenna offering improved bandwidth, radiation characteristics, and impedance matching is considered. The antenna is constructed on an FR4 substrate, with the radiating patch positioned between the substrate and a solid ground plane. A feedline strip is incorporated in the radiating patch to excite the antenna. An impedance-matching network was designed and implemented in the simulation. A multiband rectifier is utilized to convert RF power into usable output DC voltage. HSMS 2850 Schottky diodes are used to further improve efficiency. The performance of the proposed system is evaluated using Keysight Advanced Design System, taking into account metrics like return loss, radiation pattern, output voltage, and power harvesting efficiency. **The proposed rectenna achieved a bandwidth of 1.2 GHz**, with a gain of 3.56 dBi at 2.40 GHz and 8.06 dBi at 5.02 GHz. The rectenna demonstrated an output voltage of 3.65 V at an input power level of 30 dBm and -2 mV at -5 dBm input power level. A peak conversion efficiency of 83% was obtained for the overall system. The analysis of simulation and experimental results demonstrated an improved performance of the antenna in terms of increased bandwidth and enhanced power harvesting capabilities.

Keywords: Meanderline Antenna, Rectenna, Impedance Matching, RF Energy Harvesting

Večpasovna Meanderline rektena: načrtovanje in simulacija za večjo zmogljivost

Izveček: Članek predstavlja zasnovo, simulacijo in analizo nove meandrske mikropasne usmerniške antene za zbiranje energije iz frekvenčnih pasov 2,4 GHz in 5,0 GHz. Raziskava je potekala v dveh fazah. V prvi fazi je obravnavana meandrska mikropasna antena z izboljšano pasovno širino, sevalnimi lastnostmi in impedančno usklajenostjo. Antena je izdelana na podlagi FR4, pri čemer je sevalna krpica nameščena med podlago in ozemljitveno ravnino. Za vzbujanje antene je v sevalno krpico vgrajen trak napajalne linije. Za pretvorbo radijske energije v uporabno izhodno enosmerno napetost se uporablja večpasovni usmernik. Za dodatno izboljšanje učinkovitosti so uporabljene Schottkyjeve diode HSMS 2850. Delovanje predlaganega sistema je ocenjeno z uporabo sistema Keysight Advanced Design System, pri čemer so upoštevani kazalniki, kot so povratne izgube, sevalni vzorec, izhodna napetost in učinkovitost zbiranja energije. Predlagana rektena je dosegla pasovno širino 1,2 GHz z ojačitvijo 3,56 dBi pri 2,40 GHz in 8,06 dBi pri 5,02 GHz. Rektena je pokazala izhodno napetost 3,65 V pri vhodni moči 30 dBm in -2 mV pri vhodni moči -5 dBm. Največji izkoristek pretvorbe celotnega sistema je bil 83 %. Analiza simulacijskih in eksperimentalnih rezultatov je pokazala izboljšano delovanje antene v smislu povečane pasovne širine in izboljšanih zmogljivosti zbiranja energije.

Ključne besede: meandrska antena, rectenna, impedančno ujemanje, RF zbiranje energije

* Corresponding Author's e-mail: vishnunedungadi@gmail.com

1 Introduction

In recent years, there has been a growing demand for sustainable and self-powered systems in various fields, ranging from wireless sensor networks to wearable electronics. This demand has led to extensive research in the field of energy harvesting, which aims to convert ambient energy sources into usable electrical energy. Among the various energy harvesting techniques,

electromagnetic energy harvesting using antennas has garnered considerable attention due to its ability to scavenge energy from the surrounding electromagnetic field [1]. Microstrip antennas have gained significant popularity in wireless communication applications due to their compact size, low profile, and ease of integration [2-6]. However, traditional microstrip patch

antennas face challenges such as limited bandwidth and low efficiency, making them less suitable for energy harvesting applications where maximizing power transfer efficiency is of paramount importance. [7-10]. Therefore, there is a need for novel antenna designs that can address these limitations and enable efficient energy harvesting.

Recent research in the domain of RF energy harvesting has been finding an increased focus to impart multiband resonance behaviour in microstrip antennas [11-13]. This technique enables an increase in the overall efficiency of the receiving antenna without necessitating any expansion in its dimensions. [12]. This behaviour is achieved by incorporating modifications in the architecture of the antenna, such as the introduction of slots, split ring resonators, parasitic patch [12], defected ground, fractal components etc. [1, 3, 4, 14-18].

Another approach to improve the efficacy of microstrip patch antennas for energy harvesting is the incorporation of meanderline structures. Meanderline structures are periodic geometrical patterns that are introduced into the radiating patch, ground plane, or both of the antenna. These structures effectively increase the electrical length of the antenna within a limited physical footprint, thereby enhancing the antenna's bandwidth and radiation characteristics [19, 20]. The meanderline antennas offer several advantages over conventional designs, such as increased bandwidth, improved impedance matching, and enhanced radiation efficiency. These characteristics make the meanderline antenna an appropriate choice to provide efficient and compact solutions for energy harvesting in wireless communication systems.

This research article aims to investigate the application of meanderline rectennas to harvest energy from 4G, Wi-Fi and WLAN frequency bands. The main objective is to design, optimize, and characterize a meanderline microstrip patch antenna that exhibits improved performance in terms of bandwidth and power harvesting efficiency. The design parameters, such as meanderline geometry, the thickness of substrate material, and variations in the geometry of the feedline will be explored to achieve the desired antenna performance. Keysight Advanced Design Systems 2019 is used to analyze the antenna's characteristics, including return loss, radiation pattern, and power harvesting efficiency.

The primary contributions of this research work are as listed below:

a. The work focuses on the design methodology and simulation of a novel multiband slotted meanderline microstrip antenna intended for RF energy

harvesting from the surrounding environment. The obtained results are compared with existing state-of-the-art works to validate the effectiveness and performance of the proposed antenna design.

b. Parametric variations on the length, height, and width of the various elements that make up the meanderline structure are considered to identify the optimal dimensions of the overall structure

c. Suitable impedance matching network and a rectifier-doubler have been developed to convert the captured ambient RF energy into output voltage in DC form.

The proposed architecture of the microstrip meanderline rectenna is simulated and then optimised. The findings of this research article are intended to contribute to the advancement of meanderline microstrip patch rectenna as a viable solution for energy harvesting in wireless communication systems and low-power electronic devices. The improved performance and compactness of these antennas will enable the development of self-powered devices, wireless sensor networks, and IoT applications

The article is arranged as follows. Section 2 discusses the design evolution of the proposed antenna in detail. The impact of modifications in the feedline's length and width, as well as variations in the substrate's thickness, on the proposed antenna's general performance, is also examined. In section 3, an analysis of the performance of the antenna along with that of the impedance matching network and the rectifier-doubler circuit is presented. The potential and the performance of the proposed antenna is summarized in section 4.

2 Materials and Methods

The multiband antennas are extremely prevalent in RF energy harvesting applications for their capability to collect energy from different frequency bands. Meanderline antennas exhibit capabilities to address the requirements of such systems [21-26]. These antennas enables wideband operation in addition to the multiband resonance and good radiation efficiency.

To satisfy the performance criteria for energy harvesting applications, the design of the proposed antenna prioritizes the attainment of acceptable values for parameters like return loss and bandwidth. To achieve this, modifications are made to the meanderline structure of the antenna, and an impedance-matching network along with a rectifier-voltage doubler circuit is integrated. These additional components enable efficient RF-DC conversion, contributing significantly to the overall efficiency of the antenna system.

The design of the proposed rectenna is covered in two sections. In the initial stage, a patch antenna is considered with 2.4 GHz as the centre frequency to obtain the overall dimensions of the patch. The following design equations from [27] have been utilized for this purpose.

$$w = \frac{c}{2f_{res}} \sqrt{\frac{2}{1 + \epsilon_r}} \quad (1)$$

$$L = \frac{c}{2f_{res}} - 2\Delta l \quad (2)$$

$$\Delta l = 0.412h \left\{ \frac{(0.3 + \epsilon_{eff})(0.264 + w/h)}{(\epsilon_{eff} - 0.258)(0.8 + w/h)} \right\} \quad (3)$$

$$\epsilon_{eff} = \frac{\epsilon_r + 1}{2} + \frac{\epsilon_r - 1}{2} \left\{ 1 + 12h/w \right\}^{-1/2} \quad (4)$$

where w – patch width, L – patch length, c – speed of light, f_{res} – resonant frequency, ϵ_r – relative permittivity of the substrate, h – thickness of the substrate, and ϵ_{eff} – effective permittivity of the substrate.

A primitive meanderline antenna is designed initially. The meanderline structure is modified in consequent stages of the design evolution of the antenna. The Keysight Advanced Design System (ADS) software is utilized to design, simulate and analyze the antenna's performance characteristics. Each modification performed on the structure of the primitive meanderline antenna is carefully examined to understand its impact on the antenna's performance. The decision to proceed with the next modification is contingent upon the evaluation of the current design stage. Primarily, return loss (S_{11} parameter) and bandwidth are taken into account to make this decision.

Return loss is a crucial parameter that indicates the level of impedance mismatch. In antennas, a higher value of return loss points to an increased power loss due to reflection. The second parameter, bandwidth represents the range of frequency over which the antenna can function is also taken into account. These parameters are estimated at each stage of design evolution to obtain acceptable performance characteristics over the desired frequency range. A comprehensive explanation of this iterative process is provided in the results and discussion section.

The substrate material and its thickness as well as the dimensions of the feedline strip are significant in the design of the microstrip antenna. The dielectric constant,

ϵ_r , of the substrate material determines the effective wavelength, the characteristic impedance of the transmission line, and the velocity [28-30]. The resonant frequency of the antenna is influenced by the thickness of the material, with a higher thickness resulting in a lower resonant frequency. Also, a thicker substrate shall result in a narrower radiation pattern and bandwidth [5, 31, 32]. The variations in the dimensions of the feedline strip affect the performance of the antenna in a similar fashion. Improper design of the feedline strip directly contributes to impedance mismatch, reduced efficiency and introduces cross-polarisation in the radiation patterns [33-35].

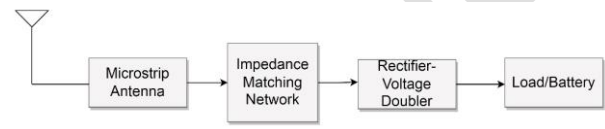







Figure 1. RF energy harvesting system - Block diagram

Proceeding with the rectenna design, the subsequent stage entails the design and integration of an impedance-matching network and a rectifier-voltage doubler circuit for the antenna. A block diagram depicting the overall RF energy harvesting system is shown in figure 1. The impedance-matching network is designed to facilitate the maximum transfer of power from the antenna to the rectification circuit. The rectification-voltage doubler circuit acts as an RF-DC converter and provides DC voltage as output to the load. In the rectifier topology, the rectifier circuit is connected to a Schottky diode. When designing an RF energy harvester, it is preferable to use a rectifier circuit based on CMOS and Schottky diodes [7, 9-11, 13-17, 33, 35].

Table 1: Progression of the design evolution of the proposed antenna.

Design Step	Antenna Design Evolution	Return Loss, S_{11} (dB)	Bandwidth (GHz)	Remarks
1	Primitive Meanderline Design 	-22.48 dB at 2.43 GHz	(2.35 - 2.65) GHz	300 MHz total bandwidth obtained. However, multiband resonance was not observed in this design.
2	Meanderline Antenna with slots of equal lengths 	-36.60 dB at 2.57 GHz	(2.51 - 2.67) GHz	A bandwidth of 570 MHz bandwidth obtained. A shift in the frequency resonance to the right was observed. Slight resonance was observed at 4 GHz and 5 GHz range
3	Meanderline antenna with slots of increasing lengths 	(4.08 – 4.29) GHz	(4.08 – 4.29) GHz	The bandwidth considerably increased to 1.21 GHz. The return loss value at the higher frequency range can be improved
4	Meanderline antenna with no slot in the first line 	(5.47 – 5.67) GHz	(5.47 – 5.67) GHz	A bandwidth of 1.09 GHz was observed. The slight reduction comes at the expense of a better return loss value over the range of frequencies
5	Meanderline antenna with slots of increasing lengths and equal slots at the turns 	-23.97 at 2.43 GHz and -18.16 dB at 4.82 GHz	(2.2 – 2.67) GHz	The overall bandwidth has increased to 1.1 GHz. Also, considerable improvement in the return loss value for the two ranges of frequency were also observed

2.1 Design progression of the proposed meanderline antenna

Table 1 illustrates the progression of design evolution of the proposed antenna. At each stage of evolution, the return loss and bandwidth are keenly observed to understand the effectiveness of the antenna design. Figure 2 depicts the S₁₁ vs frequency plot for each stage of design evolution. A primitive meanderline structure is initially considered. This was developed to harvest from the 2.4 GHz Wi-Fi band.

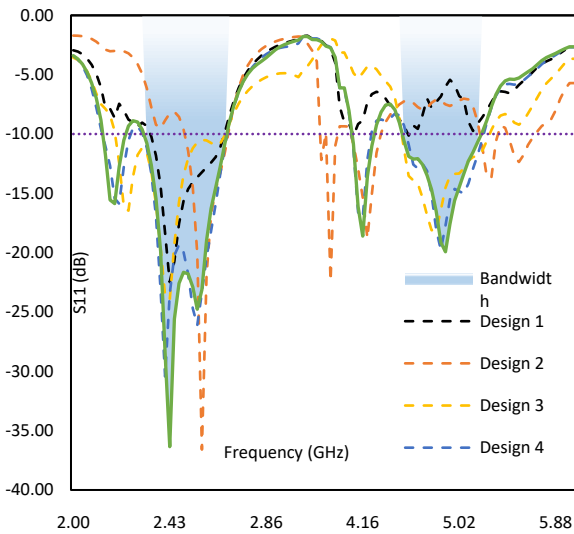


Figure 2. S₁₁ vs Frequency plots for each stage of design evolution

The primitive meanderline antenna exhibited an overall bandwidth of 300 MHz and the minimum value of return loss was observed at 2.43 GHz. In this design stage, multiband resonance was not observed. To achieve this trait, slots were introduced in the design. The simulated results showed that multiband resonance was achieved and the bandwidth had increased by 700 MHz. However, the return loss values at the higher frequencies were observed to be close to -10.00 dB reference line. This suggests that though the antenna exhibited multiband resonance, the performance is affected at the higher end of the frequency range.

To improve this condition while maintaining the overall bandwidth, the lengths of the slots were varied. It was found that by having slots of increasing lengths (traversing from bot-tom to top), the required performance of the antenna results showed that multiband resonance was achieved and the bandwidth had increased by 700 MHz. However, the return loss values at the higher frequencies were observed to be close to -10.00 dB reference line. This suggests that though the antenna exhibited multiband resonance, the performance is affected at the higher end of the frequency range. This is depicted in the third stage of design evolution.

Data from Table 1 indicates that the return loss of the proposed antenna at the third stage is higher than the return loss value obtained initially. This suggests a scope for improving the performance of the antenna still exists. Upon studying the effect of slots on the overall performance, it was found that the slot in the lowest horizontal section of the meanderline had a detrimental influence. Hence, in the 4th stage of design evolution, a design without the presence of this slot is considered. The simulated results confirmed the same. The return loss value was observed to have dropped to -30.44 dB and the bandwidth stood at 1.09 GHz at this stage.

The addition of slots in the 5th stage of design evolution is implemented to improve the overall bandwidth and the S₁₁ values in the target frequency range. This modification reduced the return loss to -36.35 dB at 2.43 GHz and improved the bandwidth by 200 MHz. The S₁₁ value at 5.5 GHz also dropped, by a very small margin, to -20.00 dB due to the addition of these slots.

Since the desired return loss and bandwidth values were achieved in this stage, design at the fifth stage of evolution was finalized. Figure 3 shows the final form of the antenna design evolution. Table 2 gives the value of lengths and widths of each component of the antenna.

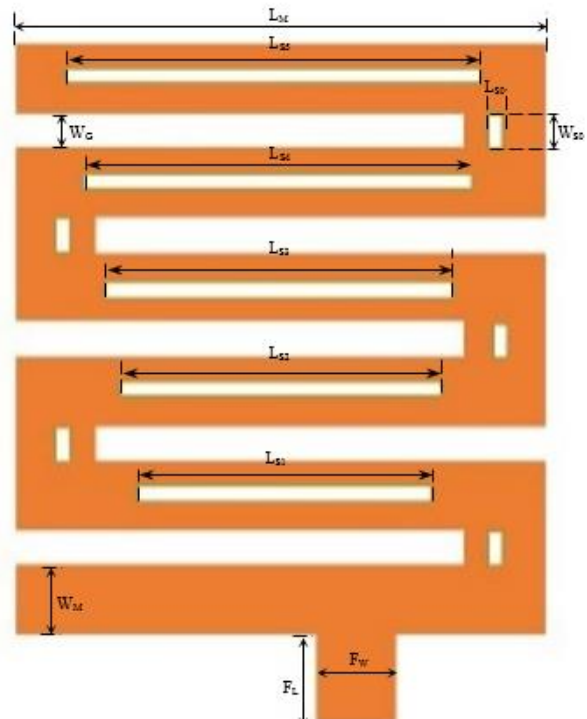


Figure 3. Final form of antenna design evolution

TABLE II. Dimensions of the proposed antenna

Parameter	Dimension (mm)
L_M	50
W_G	4
F_W	8
L_{S_4}	40
L_{S_1}	25
L_{S_0}	1.5
W_{S_0}	4
F_L	7
L_{S_3}	35
W_{S_1}	2
W_M	6
H_T	16
L_{S_5}	45
L_{S_2}	30
W_{S_2}	2

2.1.1 Effect of substrate thickness

In the proposed antenna, FR4, a flame retardant glass epoxy laminate, is used as the substrate material. FR4 is widely recognized for its stability, durability, and cost-effectiveness, making it a popular choice in various electronic applications. With the goal of identifying the ideal thickness of the substrate at which the antenna offers the desired performance characteristics, several thicknesses of the substrate are taken into consideration.

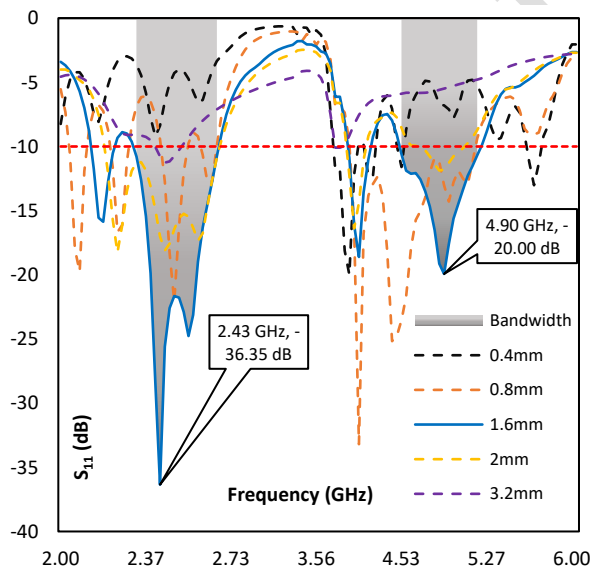


Figure 4. S11 vs Frequency plot for varying thickness of dielectric material

Figure 4 shows the performance of the proposed antenna to varying thicknesses of the substrate material. It can be understood from this plot that the reflection coefficients varied greatly with variations in the thickness of the dielectric material. The best

performance of the antenna was achieved at a thickness of 1.6 mm. At this thickness, the return loss value was observed to be -36.35 dB at 2.43 GHz and -20.00 dB at 4.93 GHz. The overall bandwidth was observed to be 1.10 GHz.

2.1.2 Effect of feedline strip

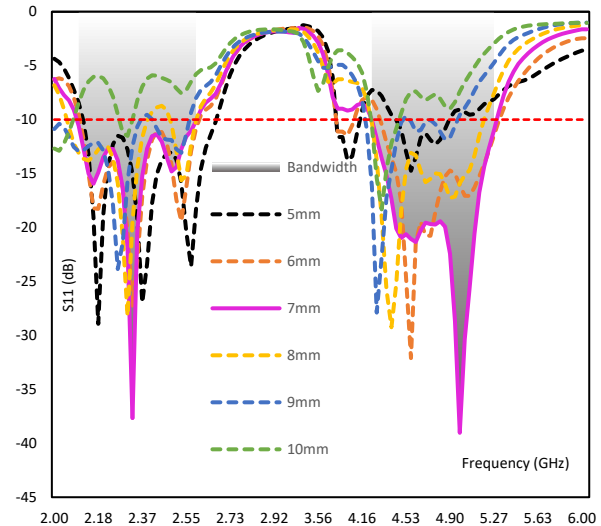


Figure 5. S11 vs Frequency plot for varying length of feedline strip

To identify the optimal length of the feedline strip in the proposed antenna, the length of the feedline is varied from 4 mm to 25 mm. The return loss versus frequency plot depicting this variation is shown in Figure 5. An analysis similar to that of the effect of variation in dielectric thickness was performed. During this analysis, close attention is given to the observed return loss and bandwidth values. The optimal performance of the antenna was obtained at a length of 7 mm of the feedline strip. Though comparable bandwidths were observed with 6 mm and 8 mm lengths, the value of S11 parameter was found to be inferior in these cases. Hence, the 7 mm length is finalized for the design.

3 Results and Discussions

The performance of the proposed antenna along with that of the impedance matching network and rectifier-doubler circuit is discussed in this section. The proposed antenna is fabricated on a double-sided copper sheet based on a FR4 substrate. A visual representation of the front and rear of the proposed antenna is shown in figure 6.

Parameters like gain, radiation pattern, efficiency, and output voltage are utilized to estimate the overall performance of the RF energy harvesting system. To evaluate the reflection coefficient (S11) of the MMA, Keysight Fieldfox Ng926A vector network analyzer was

utilized. The radiation patterns of the antenna were obtained by performing tests in an anechoic chamber.



Figure 6(a). Proposed Antenna – Front



Figure 6(a). Proposed Antenna – Rear

A transmitting horn antenna with a gain of 15 dBi along with a RF signal Generator was used for the tests. The experimental setup is as shown in figure 7. The Device-under-Test (Proposed Antenna) is placed at a distance of 1.5m from the Horn Antenna.

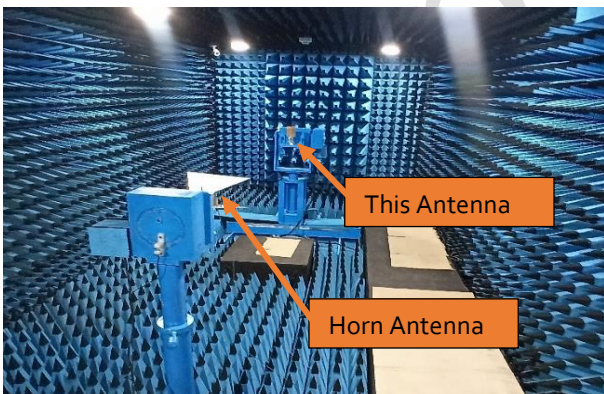


Figure 7. Experimental Setup Inside the Anechoic Chamber

3.1 Performance analysis of the proposed antenna

The return loss curve of an antenna, depicted in Figure 8, displays the relationship between return loss and frequency, integrating results from both simulation and measurement. At 2.37 GHz, the S_{11} value was recorded at -28.3 dB, while at 5.1 GHz, it measured -25.7 dB. This analysis reveals an overall bandwidth of 1.1 GHz based on the observed data.

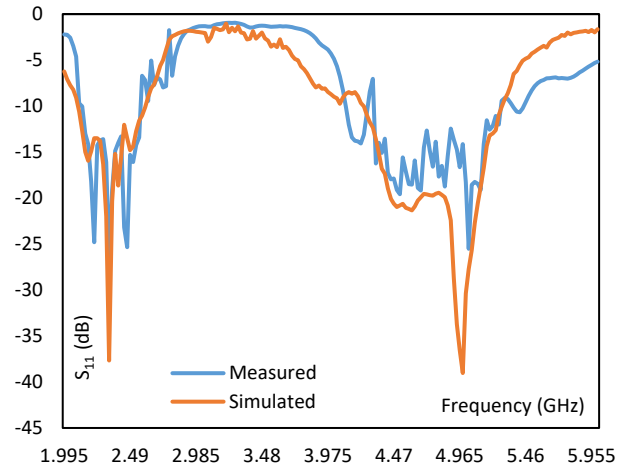


Figure 8. Simulated and Measured S_{11} vs Frequency

The variation in the value of gain of the proposed antenna across the desired frequency range can be observed in Figure 9. A maximum gain of 8.06 dBi was observed at 5.02 GHz. At 2.4 GHz, the value of gain was observed to be 3.56 dBi. The radiation properties of the proposed antenna can be better understood by examining the E-Plane and H-Plane patterns, which represent the electric field and magnetic field vectors, respectively.

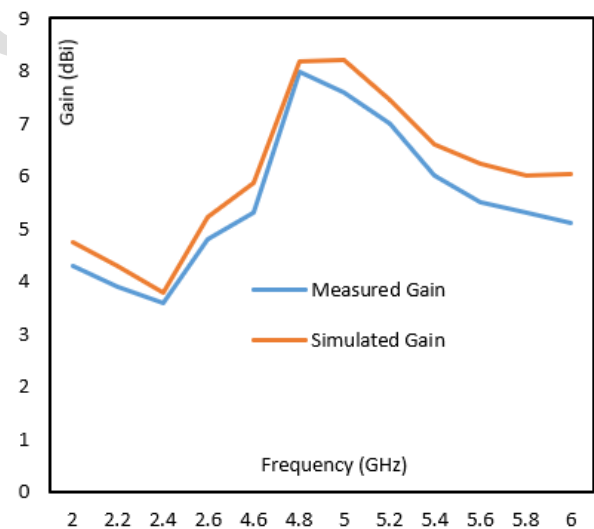


Figure 9. Gain vs Frequency of the proposed antenna

Figure 10 and Figure 11 showcase the 2D radiation patterns of the proposed antenna.

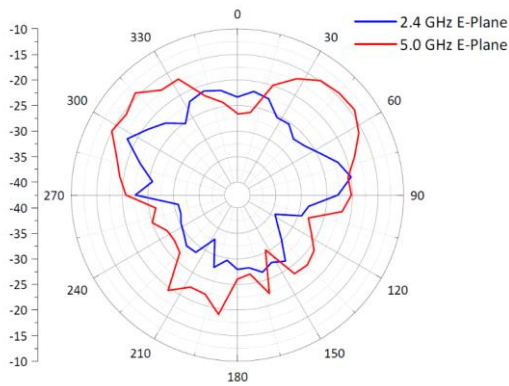


Figure 10. Measured E-Plane Pattern of the Proposed Antenna

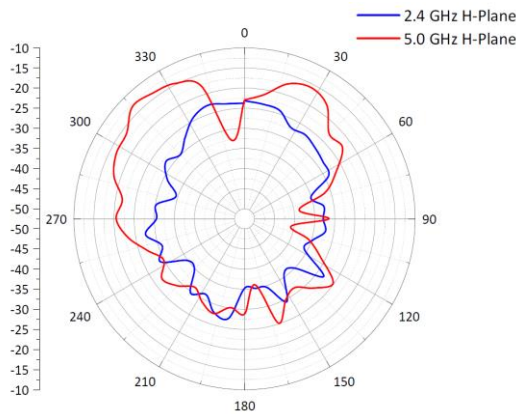


Figure 11. Measured H-Plane Radiation Pattern of the Proposed Antenna

The radiation patterns of the antenna demonstrate effective radiation. The absence of slots or defects in the solid ground ensures that there is no back propagation of the electric field. Figure 12 (a) and (b) illustrate the spatial representation of surface current distribution in the proposed antenna at frequencies of 2.4 GHz and 5.0 GHz, respectively. It is evident from this distribution that at higher frequencies, the currents are more dominant along the feedline and the lower horizontal element.

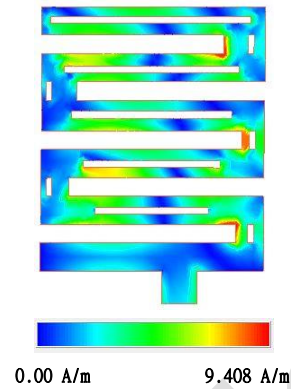


Figure 12(a)

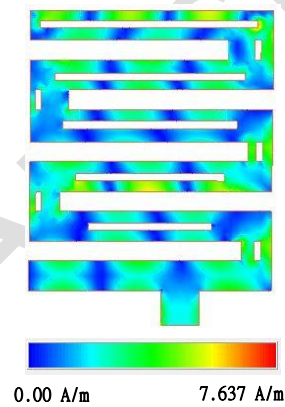


Figure 12(b)

Figure 12. Spatial representation of the surface current distribution of the proposed antenna at (a) 2.4 GHz and (b) 5.0 GHz

3.2 Impedance Matching Network

The design and analysis of an impedance-matching network is discussed in this section. The incident power on the antenna is transferred to a rectifier circuit for RF-DC conversion. The efficiency of the overall system depends greatly on the extent of power transfer between the antenna and the rectifier circuit. To effect this requirement, different types of impedance matching networks are utilised [12-16]. Typically, L, pi, and T networks are used in these scenarios.

In this work, an impedance-matching network is designed with the aid of a smith chart available in the ADS environment. The S_{11} values of the designed antenna are plotted in the smith chart as shown in Figure 13. A smith chart serves as a graphical aid employed to visualize and compute the characteristics of electrical impedance and reflection coefficients along a transmission line.

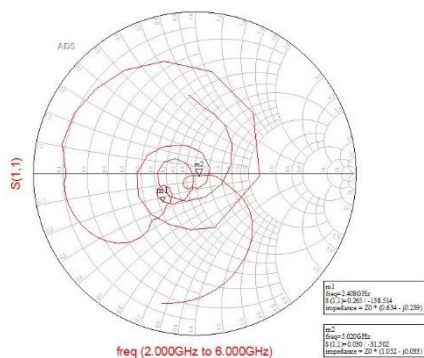


Figure 13. S11 Parameter plotted in the smith chart for the proposed antenna

From this plot, the impedance at the frequencies of interest is identified. The reference impedance is set to 50Ω. The designed impedance matching network for the proposed work is shown in Figure 14. Two inverted L-shaped L-C networks are connected to bring about the required matching characteristics.

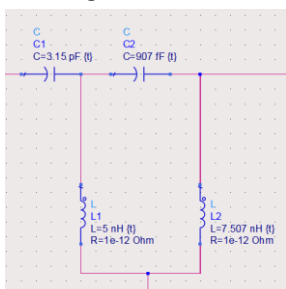


Figure 14. Impedance matching network for the proposed antenna

3.3 Multiband Rectifier-Voltage Doubler

In this section, the design, simulation, and analysis of a rectifier-voltage doubler circuit are performed using the Keysight ADS software. The purpose of this circuit is to convert the RF signal captured by the proposed micropatch meanderline antenna into an equivalent DC output voltage. Figure 15 shows the circuit diagram of the overall multiband RF energy harvesting circuit.

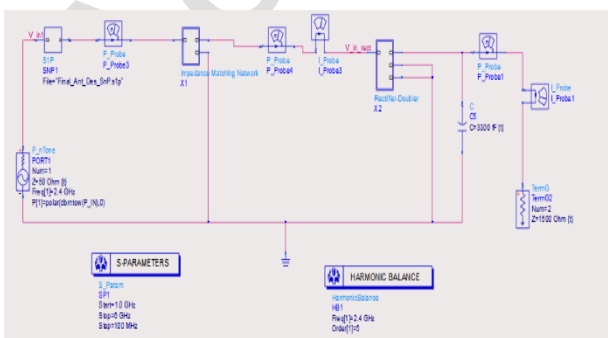


Figure 15. RF Energy Harvesting Circuit Used in ADS

The integration of impedance matching ascertains the transfer of maximum power from the antenna to the rectifier circuit. Also, the losses introduced by the two

conventional diodes have been taken into consideration. To address this issue, these diodes were replaced by HSMS 2850 series Schottky diodes. The rectifier-doubler is fabricated on the same 1.6 mm thick FR4 based double sided copper sheet. This is shown in figure 16.

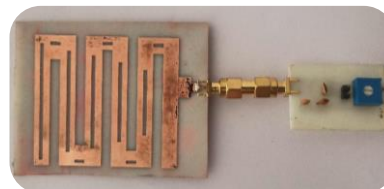


Figure 16. Proposed RF Energy Harvesting Circuit

The S11 vs frequency plot for an input power of 0 dBm is shown in Figure 17. In the simulation of the rectenna, a load resistance of 1 kΩ was utilised. The simulated results clearly show that the rectifier has been properly matched with the 50 Ω reference. The overall bandwidth of 2.1 GHz was obtained for the rectenna. Return loss values of -21.64 dB at 2.3 GHz and -21.93 dB at 5.6 GHz were observed in the simulated results.

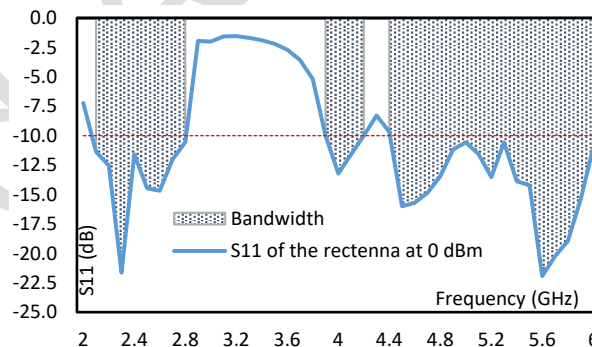


Figure 17. Reflection coefficient of rectenna at 0 dBm

The antenna is connected to the rectifier through an impedance-matching network in the simulation, facilitated by the SnP file. The file provides return loss values across the frequency range intended for the antenna's operation.

The efficiency of RF to DC conversion process performed by the rectenna is estimated using the following equation [36].

$$Efficiency, \eta = \frac{V_L^2}{R_L \times P_R} \times 100 \quad (5)$$

where R_L - load resistance, V_L - output voltage, and P_R - input power.

The proposed rectenna is shown in figure 17. Figures 18 (a) and (b) depicts the front and back view of the fabricated rectifier multiplier circuit. The impedance matching network is effected using the distributed component technique. A rectangular microstripline of 3.08 mm x 3.56 mm is cascaded with the feedline of the antenna to bring the impedance to 50 ohms. A variable resistor

is used at the load to check the performance of the rectenna at different load resistance values.

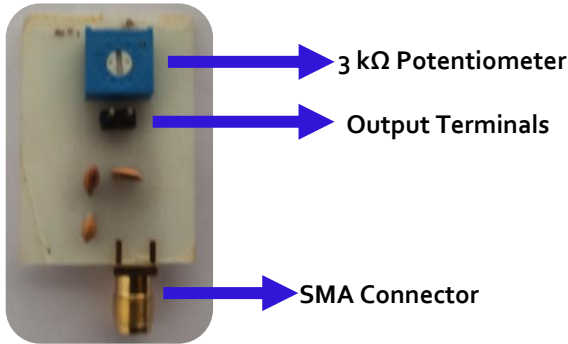


Figure 18(a). Front View

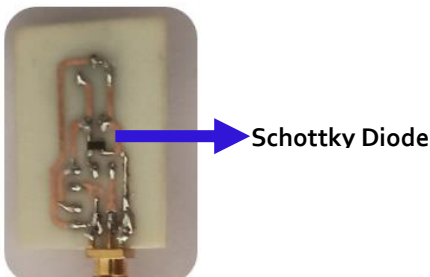


Figure 18 (b). Back View

Figure 18. Front and Back View of the Rectifier-Multiplier Circuit

Variations in load resistance affect the efficiency of the rectenna. Therefore, the input power was varied from -5 dBm to 30 dBm, and the corresponding output voltage and efficiency were noted. The efficiency versus input power and the output voltage versus input power curves of the designed rectenna at different load resistances are depicted in Figure 19 and Figure 20 respectively. From the simulation result it was inferred that a peak efficiency of 84.38% was achieved at an input power level of 21 dBm. The experimental validation showed that a peak efficiency of 77.8 % was achieved at a power level of 27 dBm.

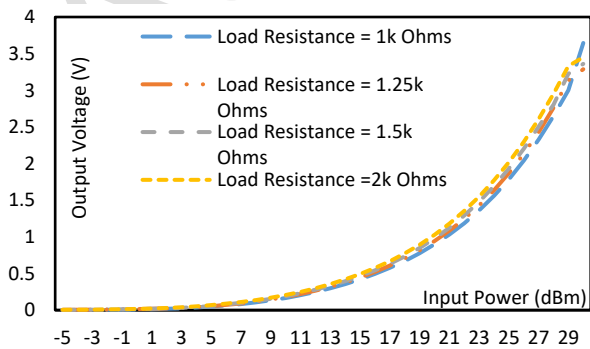


Figure 19 . Input Power vs Efficiency for Different Load Resistances

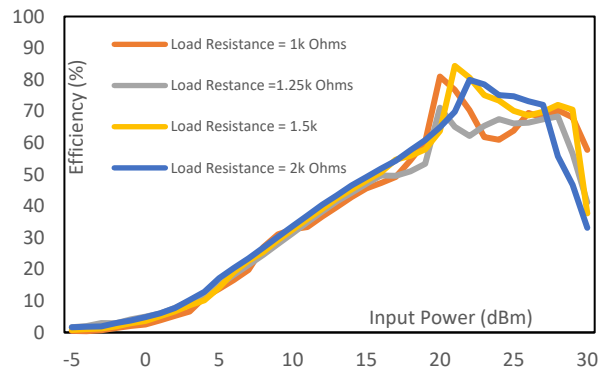


Figure 20. Output Voltage vs Input Power at Different Load Resistances

Based on the simulation results, the proposed rectenna demonstrated a minimum voltage of 2 mV at an input power of -5 dBm. Moreover, by utilizing a 1 kΩ load resistance and an input power of 30 dBm, a maximum output voltage of 3.65 V was achieved in the simulation. The experimental results exhibited that a peak output voltage of 2.84 V was achieved from the 2.4 GHz Band and an output voltage of 1.84 from the 5.0 GHz band. It is evident from the nature of the plot that the output voltage increases with an escalation in the input power and the efficiency initially increases and then decreases with an increase in the input power. This is plotted in figure 21 and 22 respectively. The efficiency dip occurs since the output voltage does not increase by a great factor with continuous increase in the input power level.

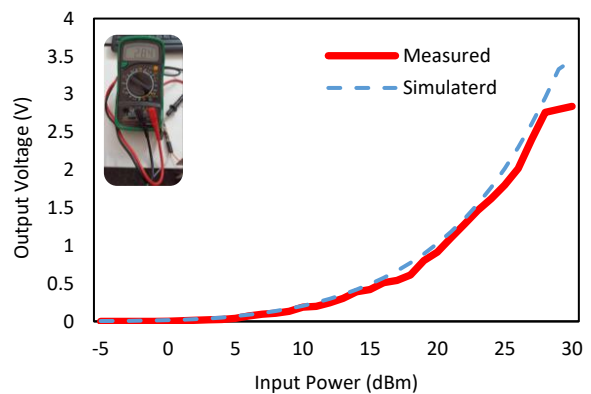


Figure 21. Input Power vs Output Voltage

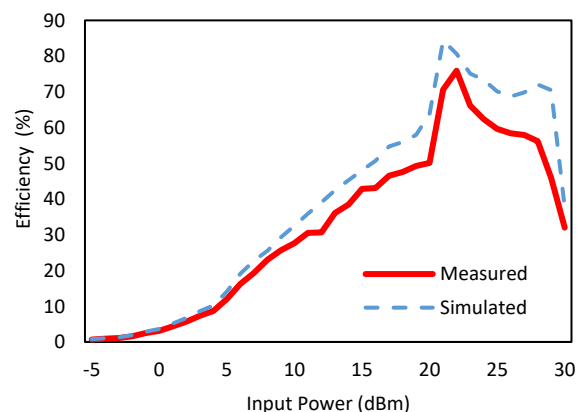


Figure 22. Input Power vs Efficiency

The proposed rectenna is compared with recent works available in the literature. The comparison is given in Table III.

TABLE III. Comparison with recent works

Ref	Frequency Band	Gain (dBi)	Peak RF-DC Efficiency (%)	BW (GHz)	Peak Output Voltage (V)
[4]	Broadband	10	72.5	0.4	4.5
[10]	2.4 GHz and 5.8 GHz	3.83	67.62	--	2.62
[7]	2.4 GHz, 3.0 GHz and 5.8 GHz	9	70	0.8	1.9
[33]	2.45 GHz	3.78	77	0.3	1.1
[25]	Broadband	4.3	88.58	2.5	10.7
This Work	2.4 GHz, 5.0 GHz	8.65	84.4	1.2 GHz	3.65

4 Conclusion

This work has successfully demonstrated the application of meanderline microstrip antennas for harvesting RF energy from wireless communication systems' frequencies. The findings highlight the potential of meanderline structures in overcoming the limitations of conventional microstrip patch antennas and improving their performance in terms of bandwidth and power harvesting efficiency. By introducing slots in the meanderline structures of the antenna's radiating patch, the overall performance of the antenna has been significantly enhanced. This improvement has led to an expanded operating bandwidth of 1.1 GHz, which is crucial for capturing a wide range of electromagnetic energy sources.

Electromagnetic simulation results revealed that the proposed antenna design exhibits improved impedance matching, reduced return loss (-36.3 dB), and enhanced radiation characteristics (8.646 dBi gain) compared to conventional designs. **The experimental results were in**

line with the simulation results. However, a slight reduction in the overall performance was observed. It is an indication of the losses encountered during the experimentation. Nonetheless, these results indicate the practical feasibility of using meanderline microstrip patch antennas to harvest RF energy from Wi-Fi and WLAN frequency bands. The improved performance and compactness of these antennas offer a promising solution for sustainable and self-powered wireless communication systems, thereby advancing energy harvesting technology.

5 Conflict of Interest

The authors of this document does not have any Conflict of Interest (COI) in publishing this paper

6 Bibliography

- [1] W. A. Khan, R. Raad, F. Tubbal, and G. Mansour, "Design of a compact antenna and rectifier for a dual band rectenna operating at 2.4 GHz and 5.8 GHz," in *INT C TELECOMMUN SYS*, 2022, pp. 1-5: IEEE. DOI: 10.1109/TSSA56819.2022.10063929.
- [2] S.-E. Adami *et al.*, "A flexible 2.45-GHz power harvesting wristband with net system output from -24.3 dBm of RF power," *IEEE T MICROW THEORY* vol. 66, no. 1, pp. 380-395, 2017. DOI: 10.1109/TMTT.2017.2700299.
- [3] N. M. Din, C. K. Chakrabarty, A. B. Ismail, K. K. A. Devi, and W.-Y. Chen, "Design of RF energy harvesting system for energizing low power devices," *PR ELECTROMAGN RES M*, vol. 132, pp. 49-69, 2012. DOI: 10.2528/PIER12072002
- [4] M.-J. Nie, X.-X. Yang, G.-N. Tan, and B. Han, "A compact 2.45-GHz broadband rectenna using grounded coplanar waveguide," *IEEE antennas wireless propagation letters* vol. 14, pp. 986-989, 2015. DOI: 10.1109/LAWP.2015.2388789.
- [5] C. Song, Y. Huang, J. Zhou, J. Zhang, S. Yuan, and P. Carter, "A high-efficiency broadband rectenna for ambient wireless energy harvesting," *IEEE T ANTENN PROPAG*, vol. 63, no. 8, pp. 3486-3495, 2015. DOI: 10.1109/TAP.2015.2431719.
- [6] H. Takhedmit, L. Cirio, S. Bellal, D. Delcroix, and O. Picon, "Compact and efficient 2.45 GHz circularly polarised shorted ring-slot rectenna," *ELECTRON LETT* vol. 48, no. 5, pp. 253-254, 2012. DOI: 10.1049/el.2011.3890.
- [7] M. Aboualalaa, I. Mansour, and R. K. Pokharel, "Energy Harvesting Rectenna Using High-gain Triple-band Antenna for Powering Internet-of-Things (IoT) Devices in a Smart Office," *IEEE T*

- INSTRUM MEAS* 2023. DOI: 10.1109/TIM.2023.3238050.
- [8] S. Agrawal, M. S. Parihar, and P. N. Kondekar, "A dual-band rectenna using broadband DRA loaded with slot," *INT J MICROW WIREL T* vol. 10, no. 1, pp. 59-66, 2018. DOI: 10.1017/S1759078717001234.
- [9] M. A. Al-Janabi and S. K. Kayhan, "Flexible vivaldi antenna based on a fractal design for RF-energy harvesting," *PR ELECTROMAGN RES M*, vol. 97, pp. 177-188, 2020. DOI: 10.2528/PIERM20073003.
- [10] K. Bhatt, S. Kumar, P. Kumar, and C. C. Tripathi, "Highly efficient 2.4 and 5.8 GHz dual-band rectenna for energy harvesting applications," *IEEE T ANTENN PROPAG LET*, vol. 18, no. 12, pp. 2637-2641, 2019. DOI: 10.1109/LAWP.2019.2946911.
- [11] Y. Chang, P. Zhang, and L. Wang, "Highly efficient differential rectenna for RF energy harvesting," *MICROW OPT TECHN LET* vol. 61, no. 12, pp. 2662-2668, 2019. DOI: 10.1002/mop.31945.
- [12] M. C. Derbal and M. Nedil, "A high gain dual band rectenna for RF energy harvesting applications," *PR ELECTROMAGN RES Lett*, vol. 90, pp. 29-36, 2020. DOI: 10.2528/PIERL19122604.
- [13] S. Divakaran and D. Krishna, "Dual-band multi-port rectenna for RF energy harvesting," *PR ELECTROMAGN RES C* vol. 107, pp. 17-31, 2021. DOI: 10.2528/PIERC20100802.
- [14] S. Chandravanshi and M. Akhtar, "An efficient dual-band rectenna using symmetrical rectifying circuit and slotted monopole antenna array," *INT J RF MICROW C E*, vol. 30, no. 4, p. e22117, 2020. DOI: 10.1002/mmce.22117.
- [15] S. Chandravanshi, S. S. Sarma, and M. J. Akhtar, "Design of triple band differential rectenna for RF energy harvesting," *IEEE T ANTENN PROPAG LET*, vol. 66, no. 6, pp. 2716-2726, 2018. DOI: 10.1109/TAP.2018.2819699.
- [16] D. Colaiuda, I. Ulisse, and G. Ferri, "Rectifiers' design and optimization for a dual-channel RF energy harvester," *J LOW POWER ELECTRON APPL* vol. 10, no. 2, p. 11, 2020. DOI: 10.3390/jlpea10020011.
- [17] A. Karampatea and K. Siakavara, "Synthesis of rectenna for powering micro-watt sensors by harvesting ambient RF signals' power," *Electronics* vol. 8, no. 10, p. 1108, 2019. DOI: 10.3390/electronics8101108.
- [18] N. Kashyap and D. Singh, "A Novel Circularly Polarized Annular Slotted Multiband Rectenna for Low Power Sensor Applications," *PR ELECTROMAGN RES B* vol. 99, pp. 103-119, 2023. DOI: 10.2528/PIERB22122606.
- [19] H. H. Ibrahim, M. S. Singh, S. S. Al-Bawri, and M. T. Islam, "Synthesis, characterization and development of energy harvesting techniques incorporated with antennas: A review study," *Sensors*, vol. 20, no. 10, p. 2772, 2020. DOI: 10.3390/s20102772.
- [20] S. Ullah, C. Ruan, M. S. Sadiq, T. U. Haq, A. K. Fahad, and W. He, "Super wide band, defected ground structure (DGS), and stepped meander line antenna for WLAN/ISM/WiMAX/UWB and other wireless communication applications," *Sensors*, vol. 20, no. 6, p. 1735, 2020. DOI: 10.3390/s20061735.
- [21] S. Muhammad, J. J. Tiang, S. K. Wong, A. Smida, M. I. Waly, and A. Iqbal, "Efficient quad-band RF energy harvesting rectifier for wireless power communications," *INT J ELECTRON COMM* vol. 139, p. 153927, 2021. DOI: 10.1016/j.aeue.2021.153927.
- [22] P. V. Naidu, A. Kumar, and R. Rajkumar, "Design, analysis and fabrication of compact dual band uniplanar meandered ACS fed antenna for 2.5/5 GHz applications," *MICROSYST TECHNOL* vol. 25, pp. 97-104, 2019. DOI: 10.1007/s00542-018-3937-8.
- [23] A. Okba, A. Takacs, H. Aubert, S. Charlot, and P.-F. Calmon, "Multiband rectenna for microwave applications," *C R PHYS* vol. 18, no. 2, pp. 107-117, 2017. DOI: 10.1016/j.crhy.2016.12.002.
- [24] N. Othman, N. Samsuri, M. Rahim, K. Kamardin, and H. Majid, "Meander bowtie antenna for wearable application," *TELKOMNIKA* vol. 16, no. 4, pp. 1522-1526, 2018. DOI: 10.12928/telkomnika.v16i4.9061.
- [25] R. Pandey, A. K. Shankhwar, and A. Singh, "An improved conversion efficiency of 1.975 to 4.744 GHz rectenna for wireless sensor applications," *PR ELECTROMAGN RES C*, vol. 109, pp. 217-225, 2021. DOI: 10.2528/PIERC20121102.
- [26] Y. Shi, Y. Fan, Y. Li, L. Yang, and M. Wang, "An efficient broadband slotted rectenna for wireless power transfer at LTE band," *IEEE T ANTENN PROPAG*, vol. 67, no. 2, pp. 814-822, 2018. DOI: 10.1109/TAP.2018.2882632.
- [27] J. D. Kraus and R. J. Marhefka, *Antennas for all applications*, 2002. [Online]. Available.
- [28] B. V. S. Suwan, W. W. G. Vidula, W. Wanniarachchi, C. H. Manathunga, and S. Jayawardhana, "The Design and Implementation of an RF Energy Harvesting System Using Dynamic Pi-Matching, Enabling Low-Power Device Activation and Energy

- Storage," *PR ELECTROMAGN RES C*, vol. 119, 2022. DOI: doi:10.2528/PIERC21121802.
- [29] D. Vital, S. Bhardwaj, and J. L. Volakis, "Textile-based large area RF-power harvesting system for wearable applications," *IEEE T ANTENN PROPAG*, vol. 68, no. 3, pp. 2323-2331, 2019. DOI: 10.1109/TAP.2019.2948521.
- [30] F. Zanon, U. Resende, G. Brandao, and I. Soares, "Energy Harvesting System Using Rectenna Applied to Wireless Powered Remote Temperature Sensing," *PR ELECTROMAGN RES C*, vol. 114, pp. 203-217, 2021. DOI: 10.2528/PIERC21060901.
- [31] K. Shafique *et al.*, "Energy harvesting using a low-cost rectenna for Internet of Things (IoT) applications," *IEEE access* vol. 6, pp. 30932-30941, 2018. DOI: 10.1109/ACCESS.2018.2834392.
- [32] H. H. R. Sherazi, D. Zorbas, and B. O'Flynn, "A comprehensive survey on RF energy harvesting: Applications and performance determinants," *Sensors* vol. 22, no. 8, p. 2990, 2022. DOI: 10.3390/s22082990.
- [33] K. Çelik and E. Kurt, "A novel meander line integrated E-shaped rectenna for energy harvesting applications," *INT J RF MICROW C E* vol. 29, no. 1, p. e21627, 2019. DOI: 10.1002/mmce.21627.
- [34] M. Koohestani, J. Tissier, and M. Latrach, "A miniaturized printed rectenna for wireless RF energy harvesting around 2.45 GHz," *INT J ELECTRON COMM* vol. 127, p. 153478, 2020.
- [35] M. Mathur, A. Agrawal, G. Singh, and S. K. J. P. I. E. R. M. Bhatnagar, "A compact coplanar waveguide fed wideband monopole antenna for RF energy harvesting applications," *PR ELECTROMAGN RES M* vol. 63, pp. 175-184, 2018. DOI: 10.2528/PIERM17101201.
- [36] R. Pandey, A. K. Shankhwar, and A. Singh, "An improved conversion efficiency of 1.975 to 4.744 GHz rectenna for wireless sensor applications," *Progress In Electromagnetics Research C* vol. 109, pp. 217-225, 2021.



Copyright © 2024 by the Authors. This is an open access article distributed under the Creative Commons Attribution (CC BY) License (<https://creativecommons.org/licenses/by/4.0/>), which permits unrestricted use, distribution, and reproduction in any medium, provided the original work is properly cited.

Arrived: 7.8.2023

Accepted: 22.04.2024

Accepted Article